Journal for Geometry and Graphics
Volume VOL (YEAR), No. NO, 1–12.

Curve Flows on ruled Surfaces

Markus Hagemann, Daniel Klawitter, and Boris Odehnal

Makus Hagemann, Daniel Klawitter
Institut für Geometrie, Fachbereich Mathematik,
Technische Universität Dresden,
Zellescher Weg 12–14, 01069 Dresden, Germany.
{*markus.hagemann,daniel.klawitter*}*@tu-dresden.de*

Boris Odehnal
Abteilung für Geometrie,
Universität für Angewandte Kunst Wien,
Oskar-Kokoschka-Platz 2, 1010 Wien, Austria.
boris.odehnal@uni-ak.ac.at

Abstract. We study special flows of curves on ruled surfaces. Closed curves on closed ruled surfaces are driven by the Gaussian curvature flow and the geodesic curvature flow. For that we use a discretization of the ruled surfaces, the curves on them, and the curvatures. In an experimental part, the problem will be attacked numerically and various types of approximations will be used.

Key Words: curve flow, curvature, geodesic flow, ruled surface, striction curve, geodesic curvature, Gaussian curvature.

MSC 2010: 53A04, 53A05, 37E35.

1. Introduction

The flow of planar curves has undergone intensive study, see *e.g.* [5, 14]. The flows that drive surfaces are usually closely related to the Mean and Gaussian curvature, see [1, 9, 11]. Especially, curve shortening flows are discussed in [4] for the planar case and the more interesting case for curves on surfaces in [6]. We shall focus on curve flows on a special class of surfaces, namely ruled surfaces.

In Section 2, we recall some basic differential geometric notions of curves just in order to familiarize the reader with the notation. Most of the facts can be found in the classical monographs on differential geometry such as [2, 15]. Some equivalent expressions for the curvature of a curve are provided. These formulas will be the basis for discrete curvature approximation methods. After that, we introduce the flow equations, which are derived by applying the heat equation to curves [13, 16].

Section 3 provides a short overview of the implementation of these curve flows. We present a not FEM-based, and therefore, more geometric method for the implementation.

ISSN 1433-8157/$ 2.50 © YEAR Heldermann Verlag, Berlin

Curves are considered as discrete sets of points. We use discrete analogues to differential geometric invariants. The development in time is approximated by a Runge-Kutta method of sufficient order. Due to numerical instabilities while calculating discrete curvatures, we present a comparison of different methods for curvature approximation, cf. [10, 14]. Furthermore, we also present an implementation of the Crank-Nicolson method (cf. [3]). In addition, we show examples for planar and spatial curve flows. As we preserve the length of the curves under the curvature flow and also under the curvature radius flow in Euclidean space, interesting topological results can be observed.

Curvature flows on ruled surfaces in the direction of the rulings are presented in Section 4. Therefore, some basic properties of ruled surfaces are described. Different equations for flows are implemented. On one hand we consider flows that depend on the Gaussian curvature and its partial derivatives. On the other hand we investigate geodesic curvature flows. Additionally, we examine flows depending on intrinsic geometric properties of the ruled surface. It turns out that all points of a given curve converge to points on the striction curve of the ruled surface. Compared to this, the geodesic flow is also studied. In the latter case the development of the curve converges to a geodesic curve on the ruled surface. Results and Examples are given in Section 5.

2. Curvature and curvature radius flows of curves

2.1. Differential geometry of curves

In the following we deal with differentiable curves

$$c(s):\ I \subset \mathbb{R} \mapsto \mathbb{R}^3$$

parametrized by their arc length. We assume that the vectors $\frac{dc}{ds} =: c'$ and $\frac{d^2c}{ds^2} =: c''$ exist at least in I and are linearly independent. Furthermore, we assume $c'' \neq 0$ for all parameters $s \in I$. Then, the *Frenet frame* (e_1, e_2, e_3) consisting of the tangent vectors e_1, the (principal) normal vector e_2, and the binormal vector e_3 is uniquely determined by

$$e_1 = c', \quad e_2 = \frac{c''}{\|c''\|}, \quad e_3 = e_1 \times e_2.$$

In order to distinguish different derivatives we shall write c' for the derivative with respect to the arc length parameter s and $\dot{c}$ indicates the derivative with respect to an arbitrary curve parameter.

We recall the *Frenet equations* (see [2, 15]) for the three-dimensional case (including the two-dimensional case with $\tau = 0$):

$$e_1' = \kappa e_2, \quad e_2' = -\kappa e_1 + \tau e_3, \quad e_3' = -\tau e_2, \tag{1}$$

$\kappa := \|c''\|$ and τ being the curvature and the torsion of c. Differential geometric properties, especially the curvature of the curve have to be approximated. Thus, we use the well-known formula (see [2, 15])

$$\kappa = \|c''\| = \frac{\|\dot{c} \times \ddot{c}\|}{\|\dot{c}\|^3}. \tag{2}$$

where c is not necessarily parametrized by its arc length.

Note that the curvature also can be expressed as the derivative of the rotation angle φ of the tangent with respect to the arc length, see [2]. So, we have

$$\kappa = \frac{d\varphi(s)}{ds}. \tag{3}$$

Furthermore, we give an expression for the curvature that will be helpful for an implicit discretization of the curvature flow (5).

$$c'' = \kappa e_2 = \frac{\dot{c} \times (\ddot{c} \times \dot{c})}{\|\dot{c}\|^4} = \frac{\langle \dot{c}, \dot{c} \rangle \ddot{c} - \langle \dot{c}, \ddot{c} \rangle \dot{c}}{\langle \dot{c}, \dot{c} \rangle^2}. \tag{4}$$

2.2. Flow equations

The flow equations we determine are derived by applying the *heat equation* to curves. In general, the heat equation for one-dimensional problems is a partial differential equation

$$\frac{\partial u}{\partial t} = \alpha \left(\frac{\partial^2 u}{\partial x^2} \right),$$

where α is called the *thermal diffusivity*, t is the parameter for the time and x denotes the place, see [16]. For curves this results in the well-known *curve shortening flow*, see [4, 5].

$$\frac{\partial c(s)}{\partial t} = \frac{\partial^2 c(s)}{\partial s^2} = \kappa e_2. \tag{5}$$

As we preserve lengths during the flow, we are dealing with, curves with constant curvature at every point are obtained. In contrast to the curve shortening flow, *i.e.*, the curvature flow, we additionally examine the *curvature radius flow*, which is given by

$$\frac{\partial c(s)}{\partial t} = \frac{1}{\kappa} e_2. \tag{6}$$

It is obvious that both flows move the points of the curve in the direction of the principal normal vector. The curvature flow ensures that the curvature of the resulting curve is constant along the curve. The curvature radius flow, however, ensures that the radius of curvature is constant all over the curve. In the planar case this always leads to a circle (see [5]) that is traced once or more times, see Figure 4 and Figure 5.

3. Implementation

In the following we give a short description of the implementation of the algorithms. The approximation in space is done by finite differences. For the time derivative a Runge-Kutta method of sufficiently high order is used in order to minimize numerical instabilities.

The given closed curve is approximated by a closed polygon with sufficiently many vertices. For the approximation of the derivatives, finite differences of order two

$$\dot{c} \approx \frac{1}{2\Delta}(c_{i-1} - c_{i+1}), \quad \ddot{c} \approx \frac{1}{\Delta^2}(c_{i-1} - 2c_i + c_{i+1})$$

and six

$$\dot{c} \approx \frac{1}{60\Delta}\big(- c_{i-3} + 9c_{i-2} - 45c_{i-1} + 45c_{i+1} - 9c_{i+2} + c_{i+2}\big),$$
$$\ddot{c} \approx \frac{1}{180\Delta^2}\big(2c_{i-3} - 27c_{i-2} + 270c_{i-1} - 490c_i + 270c_{i+1} - 27c_{i+2} + 2c_{i+3}\big),$$

are used, where Δ is the constant increment in the parameter domain of the curve. In a first attempt, we just use explicit iterative Runge-Kutta methods for the approximation of the time derivative (for details see [8]) in order to avoid solving systems of linear equations in each step. Details on Runge-Kutta methods and the techniques we used can be found in [7, 8, 13]. An explicit Euler method (order 1) as the simplest possible method, the method of Heun (order 2), the classic fourth-order method, a Runge-Kutta-Verner method (order 5) and a Runge-Kutta-Verner method (order 6) are implemented. The corresponding Butcher tableaus can be found in [8]. It is important to note that the flow equations under consideration are parabolic partial differential equations, and therefore, a condition for the space and time increment is needed, if explicit methods are used. This condition is called the *Courant-Friedrichs-Lewy* condition (CFL condition), cf. [7]

$$\frac{h}{\Delta^2} \leq C, \tag{7}$$

where C is constant and depends mainly on the partial differential equation. C is related to the minimum respectively maximum of the curvature.

3.1. Equidistant distribution of curve points

Near singularities, the distance between two neighbouring points can become very small. Therefore, we consider a second flow that distributes the points on the curve newly. This guarantees that two neighbouring points do not come too close to each other. A small distance between neighbouring points would cause a small time step because of the CFL condition (7). To avoid this effect, we use the partial differential equation

$$\frac{\partial c}{\partial t} = \frac{\langle \dot{c}, \ddot{c} \rangle}{\|\dot{c}\|^3} e_1.$$

The points of the resulting discrete curve are distributed uniformly. Figure 1 shows the effect of this flow on the curve.

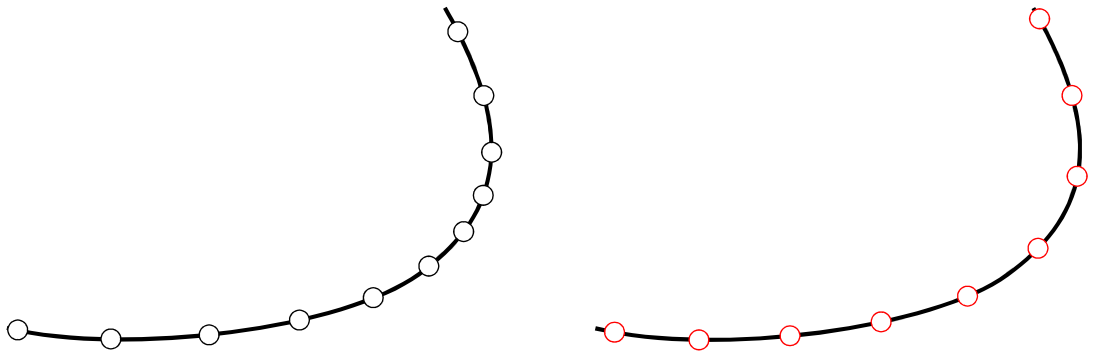

Figure 1: Old distribution (left), new distribution (right).

3.2. Approximation methods for the curvature

We use different approximations of the curvature. These are:

(i) With finite differences for $\dot{c}$ and $\ddot{c}$ we compute the discrete curvature with Eq. (2).

(ii) According to [14] we use finite differences for the angle between tangents. Let t_{i-1}, t_i, t_{i+1} be three consecutive tangents and let $\varphi^- = \angle(t_{i-1}, t_i)$, $\varphi^+ = \angle(t_i, t_{i+1})$, then Eq. (3) is approximated by

$$\kappa = \frac{1}{2d_i}\left(\varphi^+ - \varphi^-\right),$$

see Figure 2. The distance d_i is measured between the points m_{i-1} and m_{i+1} which are the midpoints of the intersections of the tangents, see also Figure 2. Note that the tangents are approximated by finite differences. Tangent lines can be skew in the spatial case. In this case, we take the intersection points of the tangents with its common normal.

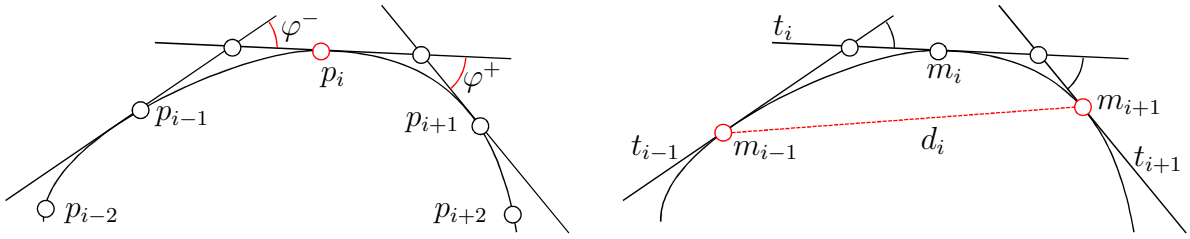

Figure 2: Finite differences for the tangent angle.

(iii) The next method follows [10]. The curvature at the point p_i is approximated by the curvature of the circle through p_i and its neighbours p_{i-1}, p_{i+1}, see Figure 3 (left).

(iv) Finally, we approximate the curvature by the curvature of a best fitting parabola. This also follows [10], see Figure 3 (right).

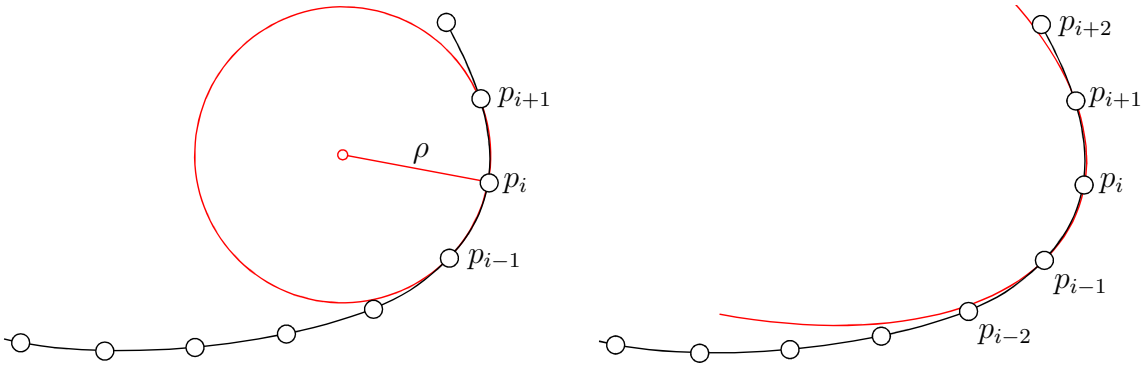

Figure 3: Curvature approximation with circle (left); curvature approximation with best fitting parabola (right).

In practice, it has turned out, that the tangent angle method for curvature approximation delivers the best results.

3.3. Crank-Nicolson method

The flow equations we are working with, are stiff differential equations, cf. [8]. Naturally, we want to formulate our discretization without a restriction to the increment of time. For this

reason an implicit method, *i.e.*, the Crank-Nicolson method, is implemented to approximate Eq. (4). This method uses the central difference quotient in time and space

$$\partial_t c_i^{n+\frac{1}{2}} = \frac{1}{\Delta_t}(c_i^{n+1} - c_i^n).$$

Furthermore, the unknown points $c_i^{n+\frac{1}{2}}$ and their derivatives are determined by the linear approximation

$$c_i^{n+\frac{1}{2}} = \frac{1}{2}\left(c_i^n + c_i^{n+1}\right).$$

Note, that the flow equation is a non-linear partial differential equation, and therefore, the Crank-Nicolson scheme is also non-linear. To avoid terms of higher order, we have modified this method by using c_i^n instead of $c_i^{n+1/2}$ for all occurring inner products

$$\partial_t c_i^{n+\frac{1}{2}} = \frac{\langle \dot{c}_i^n, \dot{c}_i^n\rangle \ddot{c}_i^{n+\frac{1}{2}} - \langle \dot{c}_i^n, \ddot{c}_i^n\rangle \dot{c}_i^{n+\frac{1}{2}}}{\langle \dot{c}_i^n, \dot{c}_i^n\rangle^2}.$$

This modification enables us to formulate and solve systems of linear equations for each coordinate

$$\left[N^2 + \mu M\right]^n c_x^{n+1} = \left[N^2 - \mu M\right]^n c_x^n,$$

with the abbreviations

$$N = D(\langle \dot{c}, \dot{c}\rangle), \quad M = N \cdot D_2^h - h \cdot D(\langle \dot{c}, \ddot{c}\rangle) \cdot D_1^h,$$

where h is the increment in space and μ is the increment in time. The matrices D_1^h and D_2^h are representations of the finite differences of first respectively second order. Furthermore, the operator D maps the inner products of all points to a diagonal matrix. Compared to explicit Runge-Kutta schemes, this method is unconditionally stable, especially in the neighbourhood of singularities. The cost of solving three systems of linear equations in each time step is lower than ensuring the CFL-condition and redistributing the points.

3.4. Curve flows in two- and three-dimensional space

Now we show some examples for the curvature flow and also for the curvature radius flow. The first example shows Pascal's limaçon, that is parametrized by

$$c(t) = \left(2\cos^2 t + \cos t,\ \sin 2t + \sin t\right)^{\mathrm{T}}.$$

In Figure 4 the resulting evolution of c is illustrated. For planar and also for spatial curves the curvature flow yields a circle, which is covered once. In contrast to this, the curvature radius flow results in a circle that is covered twice. So this flow does not influence topological properties like the winding number.

We apply the curvature flow to a spatial curve c on a torus of major radius 2 and minor radius 1:

$$c = ((2 + \cos 2u)\cos u, (2 + \cos 2u)\sin u, \sin 2u)^{\mathrm{T}}.$$

In Figure 6 the evolution of this curve under the curvature flow (5) is illustrated for several time steps.

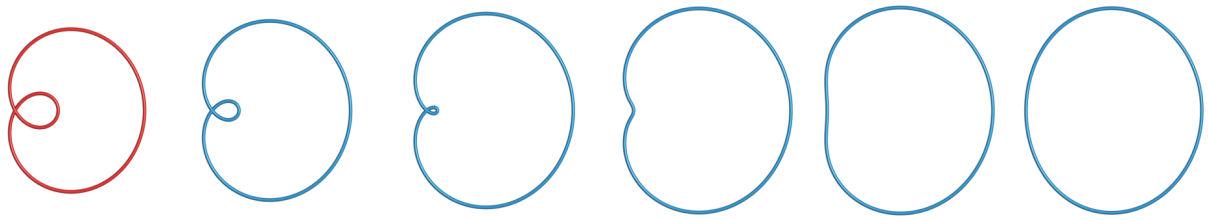

Figure 4: Planar curvature flow with Crank-Nicolson method, initial curve (red), timesteps 1, 7, 11, 12, 51, 101.

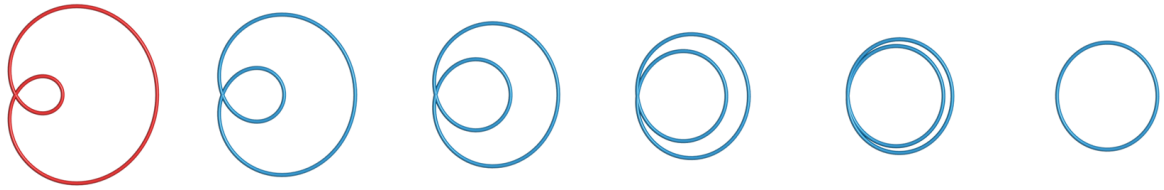

Figure 5: Planar curvature radius flow with Runge-Kutta method, initial curve (red), timesteps 1, 5, 9, 15, 21, 61.

4. Curvature and curvature radius flows on ruled surfaces

We follow [12] and collect all necessary facts on ruled surfaces. A surface is called a *ruled surface* if it carries a one-parameter family of straight lines. Thus, it can be parametrized by

$$f(u,v) = c(u) + v \cdot e(u),$$

where $c: I \to \mathbb{R}^3$ is a *directrix* and $e: I \to S^2$ is called the *spherical image of the ruled surface* determining the direction of the rulings.

We denote the partial derivatives of f by f_u and f_v. The *striction curve* γ of a ruled surface

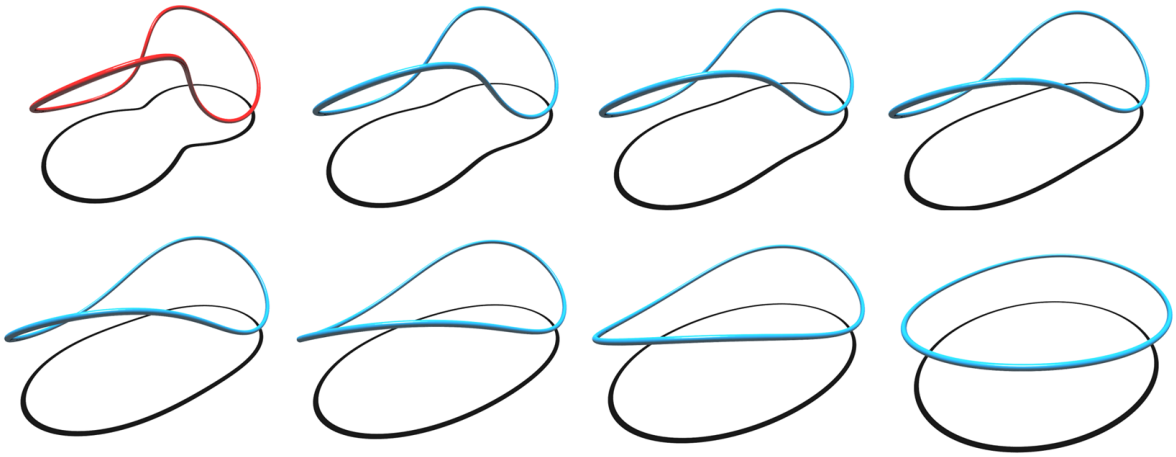

Figure 6: Curvature flow (spatial curve).

is the locus of maximal Gaussian curvature on a ruled surface and can be parametrized by

$$\gamma(u) = c - \frac{\langle \dot{c}, \dot{e} \rangle}{\langle \dot{e}, \dot{e} \rangle} e. \tag{8}$$

We call a point of the ruled surface *singular* if the partial derivatives f_u and f_v are linearly dependent.

The *parameter of distribution* δ for a ruled surface describes the winding speed of the tangent planes winding about the ruling, cf. [12]. It can be determined by

$$\delta := \frac{\det(\dot{c}, e, \dot{e})}{\|\dot{e}\|^2},$$

which only depends on u. The *Gaussian curvature* can be computed with Lamarle's formula (see [12]) as

$$K = -\frac{\delta^2}{(\delta^2 + v^2)^2} < 0.$$

Note that K is a function only in v at any fixed generator. Another differential geometric property is the *geodesic curvature* of a curve on a (ruled) surface

$$\kappa_g = \frac{\det(n, \dot{c}, \ddot{c})}{\|\dot{c}\|^3},$$

where n denotes the unit normal of the surface.

4.1. Curve flows on ruled surfaces

We treat curve flows on ruled surfaces in the direction of the rulings. Therefore, the equation of the *Gaussian flow* reads

$$\frac{\partial c}{\partial t} = e \cdot \frac{\partial}{\partial v} \ln K = e \cdot \frac{\partial K}{\partial v} \frac{1}{K}, \tag{9}$$

with e being the spherical image of the ruled surface. Hence, we examine the Gaussian curvature on every ruling. The flow forces the curve in the direction of increasing Gaussian curvature.

There is another flow equation we are dealing with: It is the *geodesic flow* which can be written as

$$\frac{\partial c}{\partial t} = \kappa_g e, \tag{10}$$

where κ_g is the geodesic curvature of c with respect to the ruled surface. In this case the points of the curve are forced in the direction of decreasing geodesic curvature. At this point the Gaussian curvature is calculated analytically, because a parametrization of the ruled surfaces is known. In contrast to this, the geodesic curvature is approximated. The aim is to show that every curve converges to the striction curve under the Gaussian flow, or to a geodesic curve under the geodesic flow, respectively. The advantage of this method is that for every set of given lines the striction curve can be approximated by the Gaussian flow applied to an arbitrary discrete curve on this discrete ruled surfaces.

4.2. Convergence

Now we are able to state and prove:

Theorem 4.1. *The Gaussian curvature flow of a curve on a ruled surfaces in the direction of the ruling* (9) *converges to the striction curve.*

Proof. The quotient $\frac{K_v}{K}$, and therefore, the flow of the Gaussian curvature can be expressed by

$$\frac{K_v}{K} = -4\frac{\langle f_u, f_{uv}\rangle}{\langle f_u, f_u - \langle f_u, f_v\rangle f_v\rangle}.$$

This equation can be interpreted geometrically. The projection of the derivative of the curve is compared with the derivative of the spherical image of the ruled surface. If the numerator is equal to zero, the flow stops and the striction curve is reached at this point

$$\langle f_u, f_{uv}\rangle = \langle c_u + ve_u, e_u\rangle \stackrel{!}{=} 0 \Rightarrow v = -\frac{\langle c_u, e_u\rangle}{\langle e_u, e_u\rangle}.$$

The parameter v corresponds to the parameter of the striction curve, see Eq. (8). □

We suspect a curve under the geodesic flow on the ruled surface in the direction of the ruling to converge to a closed geodesic on the ruled surface. Due to numerical errors produced by the method we use, the curve evolves to the shortest closed geodesic curve on the ruled surface. Analytically, the solution is one geodesic curve and not the shortest closed geodesic curve in general. This conjecture is based on observations we made, see Section 5.

5. Examples

Now we present a collection of examples for curve flows on ruled surfaces. The first example is one of the two ruled surfaces in one-sheeted hyperboloid. The ruled surface within the hyperboloid is given by the parametrization:

$$f(u,v) = (a\cos u, b\sin u, 0)^{\mathrm{T}} + v\cdot(-a\sin u, b\cos u, c)^{\mathrm{T}}/\sqrt{a^2\sin^2 u + b^2\cos^2 u + c^2}.$$

In the following, we choose $a = 2$, $b = 3$, and $c = 3.7$. It is well-known that the striction curve of one regulus on a (one-sheeted) hyperboloid is a rational space curve of degree 4 unless the quadric is not a quadric of revolution. We have to remark that the Gaussian flow we are using is not a flow defined by properties of the curve. It just depends on the surface. Thus, it could be called a *pseudoflow*. The effect of this flow is visualized in Figure 7 (left). In Figure 7 (right) the development of an arbitrary curve under the geodesic flow is visualized.

All singular points of a ruled surface are contained in the striction curve. The Gaussian curvature at these points is not defined. This is the reason why the flow can develop singularities. If the calculated curve gets too close to singularities, difficulties in the computation may occur.

To convince that a closed curve undergoing the geodesic flow converges to the shortest closed geodesic curve on the ruled surface, we compute the length of the resulting curve in every time step. For the one-sheeted hyperboloid the shortest closed geodesic curve is the ellipse $(a\cos u, b\sin u, 0)^{\mathrm{T}}$.

Since computing the circumference of an ellipse results in an elliptic integral which cannot be determined exactly we give an approximated circumference by $l = 15.865$. Figure 8

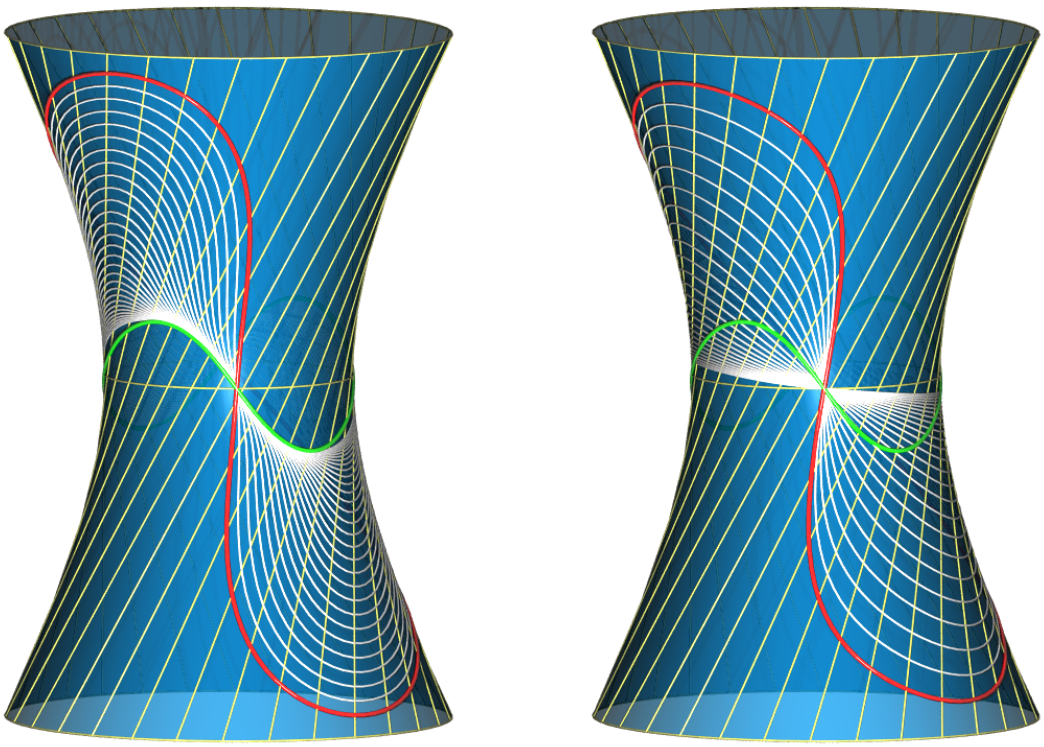

Figure 7: Gaussian flow on hyperboloid (left), geodesic flow (right), initial curve (red), evolution curves (white), striction curve (green).

visualizes the evolution of the length of the curve under the geodesic flow, denoted by $l(c)$, together with the length l of the exact shortest closed geodesic curve. The length of the flowing curve converges to the circumference of the ellipse.

Furthermore, we examine the total geodesic curvature $\int \kappa_g \, \mathrm{d}s$ for each curve. Since we suppose that the resulting curve is a geodesic, the total geodesic curvature has to converge to zero, see Figure 8.

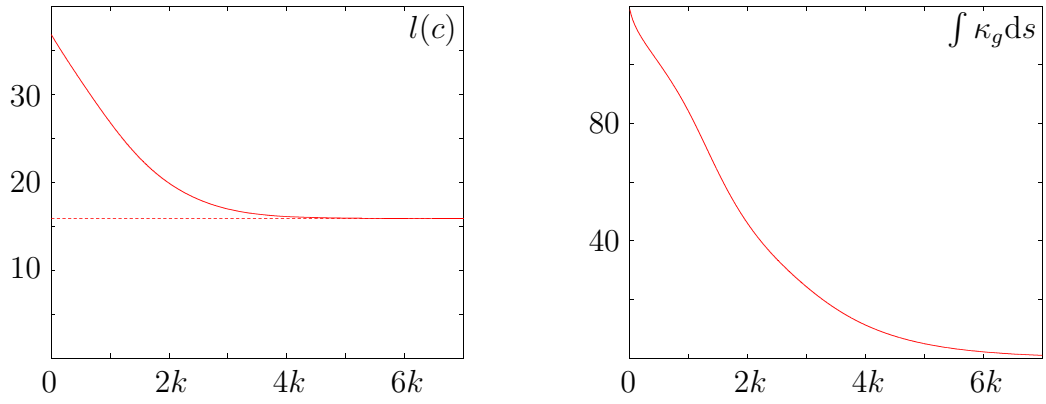

Figure 8: Evolution of the length of the curves (left), evolution of the total geodesic curvature (right) over 7000 time steps.

Our next example is chosen specifically. The ruled surface is parametrized by

$$f(u,v) = (a\sin u, 0, c)^{\mathrm{T}} + v \cdot (-a\sin u, b\cos u, -2c)^{\mathrm{T}}.$$

Its striction curve has four singular points. For our numerical example, we choose $a = 4$, $b = 4$, $c = 4$. Figure 9 shows the result of both flows.

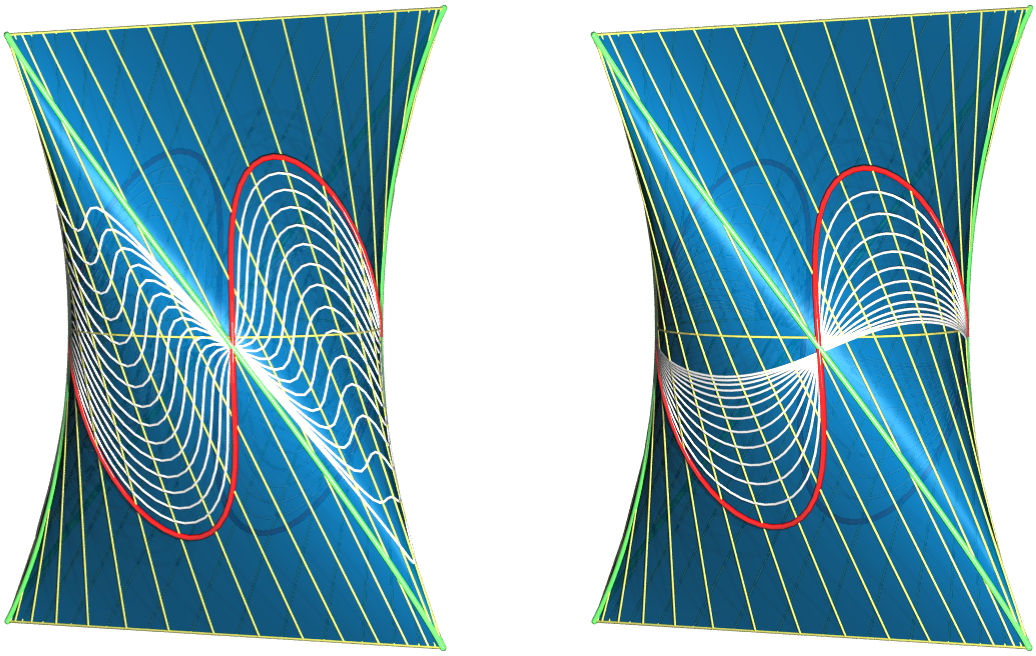

Figure 9: Gaussian flow (left), geodesic flow (right), initial curve (red), evolution curves (white), striction curve (green).

6. Conclusion and further research

We derived flow equations from the heat equation and showed different implementation methods. Due to numerical instabilities different approximation methods for the curvature were presented. We have presented examples of different flows of curves on ruled surfaces. It turned out that curves under the Gaussian curvature flow converge to the striction curve of the ruled surface. Closed curves undergoing the geodesic flow converge to a geodesic on the ruled surface, possibly to the shortest closed geodesic on the surface.

However, a discrete analogue of the Gaussian curvature could also be of interest. Further, one could ask for flows of ruled surfaces preserving the rulings. Flows that change the distribution of rulings within a given ruled surface could also be studied. The mathematical formulation would be of interest.

Acknowledgments

This work was supported by the research project "Line Geometry for Lightweight Structures", funded by the DFG (German Research Foundation) as part of the SPP 1542.

References

[1] B. Andrews: *Gauss curvature flow: the fate of rolling stones.* Invent. math. **138** (199), 151–161.

[2] M.P. do Carmo: *Differential geometry of curves and surfaces.* Prentice-Hall, 1976.

[3] J. Crank, P. Nicolson, and D.R. Hartree: *A Practical Method for Numerical Evaluation of Solutions of Partial Differential Equations of the Heat-Conduction Type.* Proc. Cambridge Phil. Soc. **43** (1947), 50–67.

[4] K.-S. Chou, X.-P. Zhu: *The Curve Shortening Problem.* Chapman & Hall/CRC, 2001.

[5] M.E. Gage: *Curve shortening makes convex curves circular.* Invent. math. **76** (1984), 357–364.

[6] M.E. Gage: *Curve shortening on surfaces.* Ann. Sci. L'École Normale Supérieure **23** (1990), 229–256.

[7] C. Grossmann, H.-G. Roos, and M. Stynes: *Numerical Treatment of Partial Differential Equations.* Springer-Verlag, Berlin, Heidelberg, 2007.

[8] M. Hermann: *Numerik gewöhnlicher Differentialgleichungen.* Oldenbourg-Verlag, München-Wien, 2004

[9] G. Huisken: *Flow by Mean Curvature of Convex Surfaces into Spheres.* J. Diff. Geom. **20** (1984), 237–266.

[10] T. Lewiner, J.D. Gomes jr., H. Lopes, and M. Craizer: *Curvature and torsion estimators based on parametric curve fitting.* Computers and Graphics **29** (2005), 641–655.

[11] C. Lu, Y. Cao, and D. Mumford: *Surface Evolution under Curvature flows.* Journal of Visual Communication and Image Representation **13** (2002), 6581.

[12] H. Pottmann, J. Wallner: *Computational line geometry.* Springer-Verlag, Berlin, 2001.

[13] G.W. Recktenwald: *Finite-Difference Approximations to the Heat Equation.* Available at `http://www.f.kth.se/jjalap/numme/FDheat.pdf`, last access: 03/2011.

[14] S. Roberts: *A Line Element Algorithm for Curve Flow Problems in the Plane.* Centre for Mathematical Analysis, Australian National University, 1989.

[15] M. Spivak: *A comprehensive introduction to differential geometry.* Publish or Perish, 3^{rd} edition, 1999.

[16] R.K.M. Thambynayagam: *The Diffusion Handbook: Applied Solutions for Engineers.* McGraw-Hill Professional, 2011.

Received